Rojas-Lema, S.; Nilsson, K.; Trifol, J.; Langton, M.; Gómez-Caturla, J.; Balart, R.; Garcia-Garcia, D.... (2021). Faba bean protein films reinforced with cellulose nanocrystals as edible food packaging material. Food Hydrocolloids. 121. https://doi.org/10.1016/j.foodhyd.2021.107019

"Faba bean protein films reinforced with cellulose nanocrystals as edible food packaging material"

Sandra Rojas-Lema[a], Klara Nilsson[b], Jon Trifol[c], Maud Langton[b], Jaume Gomez-Caturla[a], Rafael Balart[a], Daniel Garcia-Garcia[a]*, Rosana Moriana[b,c,d]

[a] *Instituto de Tecnología de Materiales (ITM)*
Universitat Politècnica de València (UPV)
Plaza Ferrándiz y Carbonell 1, 03801, Alcoy, Alicante (Spain)

[b] *Department of Molecular Sciences*
Swedish University of Agricultural Sciences (SLU)
Box 7051, SE-750 07, Uppsala (Sweden)

[c] *Department of Fibre and Polymer Technology, School of Engineering Sciences in Chemistry, Biotechnology and Health.*
Royal Institute of Technology (KTH)
SE-100 44, Stockholm (Sweden)

[d] *RISE Bioeconomy and Health*
Research Institute of Sweden (RISE)
Drottning Kristinas väg 61, SE-114 28, Stockholm (Sweden)

* Corresponding author: D. Garcia-Garcia
E-mail: dagarga4@epsa.upv.es
Tel.: (+34) 96 652 84 34
Fax: (+34) 96 652 84 33

Abstract

In the present work, transparent films were obtained by the solution casting method from faba bean protein isolate (FBP), reinforced with different cellulose nanocrystals (CNCs) content (1, 3, 5 and 7 wt%), obtained by acid hydrolysis of pine cone, and using glycerol as plasticizer. The influence of different CNCs loadings on the mechanical, thermal, barrier, optical, and morphological properties was discussed. Microstructurally, the FTIR and FESEM results corroborated the formation of intramolecular interactions between the CNCs and proteins that lead to more compact and homogeneous films. These interactions had a positive influence on the mechanical strength properties, which is reflected in higher tensile strength and Young's modulus in reinforced films with respect to the control film, resulting in stiffer films as the CNCs content increases. Thermal stability of the FBP films was also improved with the presence of CNCs, by increasing the characteristic onset degradation temperature. In addition, the linkages formed between the CNCs, and proteins reduced the water affinity of the reinforced films, leading to a reduction in their moisture content and water solubility, and an increase in their water contact angle, obtaining more hydrophobic films as the CNCs content in the matrix increased. The addition of CNCs in the FBP film also considerably improved its barrier properties, reducing its water vapour transmission rate (WVTR) and oxygen transmission rate (OTR). The present work shows the possibility of obtaining biobased and biodegradable films of CNC-reinforced FBP with improved mechanical, thermal and barrier properties, and low water susceptibility, which can be of great interest in the food packaging sector as edible food packaging material.

Keywords: Faba beans; proteins films; cellulose nanocrystals (CNCs); food packaging; pine cone.

1. INTRODUCTION

In recent years, the worldwide consumption of plastics has increased in a remarkable way, mainly due to its high versatility and low price. Only in Europe there was a total production of 57.9 million tonnes in 2019, with the packaging industry being the main consumer with a 39.6% of the total (Plastics Europe, 2020). The high consumption of plastics generates a large amount of waste that causes serious environmental problems, especially when used as single-use packaging materials. This has led to an increase in environmental concern in society which, together with petroleum depletion, has led to a considerable increase in the research and development of new, more environmentally friendly materials capable of replacing traditional synthetic plastics (Liminana, Garcia-Sanoguera, Quiles-Carrillo, Balart, & Montanes, 2018). Among the sustainable materials that have received the most attention, biodegradable polymeric films from renewable sources that are abundant in nature such as proteins, lipids and polysaccharides, have positioned as an actual alternative to synthetic polymer films, and are characterized by their biodegradability, wide availability, and low cost (Zhang, et al., 2016). Protein films are characterized by their non-toxicity, biodegradability and good barrier properties to oxygen, lipids and flavourings (Reddy, Jiang, & Yang, 2012). However, they have a number of drawbacks compared to synthetic polymers that limit their massive use in sectors such as packaging. Among these disadvantages, it is worthy to note their low mechanical strength, poor water vapour barrier properties and high water sensitivity due to the highly hydrophilic nature of the proteins (Bourtoom, 2009). Although these properties highly depend on the protein structure and the method of film preparation (Salgado, Ortiz, Petruccelli, & Mauri, 2010).

Legume seeds are a cheap source of protein with high nutritional value, which makes them an interesting raw material for use in the manufacture of bio-based materials for the packaging sector due to their sustainability (Makri, Papalamprou, & Doxastakis, 2005). One of the most consumed legumes worldwide is faba bean (*Vicia Faba L.*), which is characterized by its low cost and high quality protein content, which can contain up to 27.34% protein (dry weight), depending on the cultivation conditions and the variety. (Samaei, et al., 2020). Faba bean has long been a basic food

staple in Middle Eastern and Southeast Asian countries, however, its main use has been as a livestock feed, although it has also been used as a cover crop to restore nitrogen content and prevent soil erosion (Nivala, Nordlund, Kruus, & Ercili-Cura, 2020; Vioque, Alaiz, & Girón-Calle, 2012). This makes it an excellent raw material for protein extraction for use as films in the food packaging industry. However, currently, the use of faba bean proteins to produce biodegradable films is still very limited. Some works such as those carried out by Saremnezhad *et al.* (Saremnezhad, Azizi, Barzegar, Abbasi, & Ahmadi, 2011) and Montalvo-Paquini *et al.* (Montalvo-Paquini, Rangel-Marrón, Palou, & López-Malo, 2014) analyzed the effect of different pH values, and plasticizer content of film forming solution on the physical and chemical properties of faba bean protein films. On the other hand, Hopkins *et al.* (Hopkins, Stone, Wang, Korber, & Nickerson, 2019) observed that faba bean protein films with 50% glycerol content, had better tensile strength and opacity and lower water permeability than protein films obtained from other legumes such as peas, lupins, lentils, and soybeans.

On the other hand, the formulation of protein films requires the use of plasticizers to reduce their brittleness and increase their functionality. The plasticizer molecules interact by hydrogen bonding with amino-acid groups in protein chains, thus reducing the intermolecular forces between them, resulting in an increase in their mobility, which translates into an increase in the flexibility, toughness and tear strength of the films (Aguirre, Borneo, & León, 2013; Tian, Guo, Xiang, & Zhong, 2018). Some of the most commonly used plasticizers for the manufacture of protein films are sorbitol, polyethylene glycol and glycerol, being glycerol one of the most effective for the production of stable, flexible and less brittle films (Pérez, Piccirilli, Delorenzi, & Verdini, 2016; Ramos, et al., 2013). Glycerol is one of the most important by-products of biodiesel production, which is generated in large amounts due to the remarkable increase in biodiesel production, becoming a waste product with an associated economic and environmental cost (Rosa, et al., 2010; Tong, Luo, & Li, 2015). Glycerol represents approximately 10 wt% of total biodiesel production (Yang, Hanna, & Sun, 2012). Therefore, the use of glycerol as plasticizers in protein films, in addition to increasing the ductile mechanical properties of the

107 films, can be an effective alternative to convert a by-product of the biodiesel industry into a high
108 value-added product (Ye, Xiu, Shahbazi, & Zhu, 2012).

109 One of the approaches to overcome the above-mentioned drawbacks of protein films is the use of
110 nanoparticles. The use of small amounts of nanoparticles has shown good potential to improve
111 the mechanical and barrier properties of protein films (Calva-Estrada, Jiménez-Fernández, &
112 Lugo-Cervantes, 2019). Inorganic nanoparticles such as montmorillonite (Azevedo, et al., 2018;
113 Azevedo, Silva, Pereira, da Costa, & Borges, 2015; Kumar, Sandeep, Alavi, Truong, & Gorga,
114 2010; Pereira, Carneiro, Assis, & Borges, 2017), TiO_2 (Fathi, Almasi, & Pirouzifard, 2019; Li, et
115 al., 2011; Y. Liu, et al., 2019), halloysite nanotubes (Kang, Liu, Zhang, & Li, 2017; X. Liu, et al.,
116 2017), or carbon nanotubes (Xiang, Guo, & Tian, 2017) have been successfully employed to
117 reduce the drawbacks of protein films. However, the use of renewable and biodegradable
118 nanoparticles has gained relevance in recent years due to their greater environmentally
119 friendliness. In this way, cellulose nanocrystals (CNCs) obtained from agroforestry residues are
120 considered one of the most promising reinforcing agents due to their biodegradability, abundance,
121 variety, chemical modification capacity and price (Garcia-Garcia, Lopez-Martinez, Balart,
122 Strömberg, & Moriana, 2018). Cellulose nanocrystals consist of highly crystalline rod-like
123 particles, obtained from biomass, usually by acid hydrolysis, with dimensions of around 10-20
124 nm in width and several hundred nanometers in length, giving rise to high aspect ratios (Xu, et
125 al., 2013). CNCs are characterized by high strength, high elastic modulus and low density
126 (Moriana, Vilaplana, & Ek, 2016), despite their physico-chemical properties depend on the
127 cellulose source, and on synthesis process conditions (Silvério, Neto, Dantas, & Pasquini, 2013;
128 Slavutsky & Bertuzzi, 2014). CNCs are also characterized by good compatibility with hydrophilic
129 polymers (Han, Yu, & Wang, 2018). The effect of CNC incorporation has been previously studied
130 in soy (González & Igarzabal, 2015; Han, et al., 2018; Yu, et al., 2018; Zhang, et al., 2016), whey
131 (Qazanfarzadeh & Kadivar, 2016), amaranth (Condés, Añón, Mauri, & Dufresne, 2015), or canola
132 (Osorio-Ruiz, Avena-Bustillos, Chiou, Rodríguez-González, & Martinez-Ayala, 2019) protein
133 films, showing that the presence of nanoparticles in the protein matrix leads to intramolecular

interactions between both phases, resulting in more compact films with better mechanical properties and better barrier properties.

The main objective of the present work is to evaluate the effect of the incorporation of different CNC content extracted from pine cone (1, 3, 5 and 7 wt%) on the mechanical properties, thermal stability, barrier properties, optical properties, water susceptibility (moisture content, contact angle and water solubility) and the microstructure on glycerol-plasticized faba bean protein-based biodegradable films.

2. EXPERIMENTAL

2.1 Materials

Faba beans used in this work (*Gloria* variety) were supplied by RISE (Research Institutes of Sweden). Pine cones (*Pinus Pinea*) were collected from a local pine forest in Alicante (Spain). Sodium hydroxide (NaOH, 99.0% purity) and hydrochloric acid (HCl, 36% purity) were supplied by VWR (Darmstadt, Germany). Glycerol was purchased from POCH S.A. (Gliwice, Poland).

2.2 Faba bean protein isolation

The faba bean protein (FBP) isolation was done following the method described by Langton *et al.* (Langton, et al., 2020) with some modifications. First, the faba beans were dehulled with a dehuller, and the beans were milled in a rotary mill from Brabender (Duisburg, Germany) with a 1.5 mm mesh screen. Subsequently, faba bean flour was mixed in distilled water at a ratio 1:10 (w/v) and the pH of the obtained solution was adjusted to 9.0 using 2 M NaOH to increase solubility of the protein. The suspension was stirred at room temperature for 1 h, and then was centrifuged in a Sorvall Lynx 6000 centrifuge from Thermo Scientific (Langenselbold, Germany) at 3700 G for 30 min and 18 ºC. The pH of supernatant was adjusted to 4.0 using 1 M HCl to precipitate the protein, stirred at room temperature for 1.5 h and centrifuged at 3700 G for 30 min and 18 ºC. The precipitates were collected and re-dispersed in distilled water at a ratio 1:10 (w/v). The suspension was adjusted to pH 4 and centrifuged again with the same described conditions. Finally, the precipitate protein was frozen and lyophilized to obtain FBP.

2.3 Preparation of pine cone nanocrystals

Pine cone nanocrystals were obtained by acid hydrolysis according to our previous work (García-García, Balart, Lopez-Martinez, Ek, & Moriana, 2018). Briefly, grinded pine cone particles were first subjected to an alkaline treatment in a 4.5% NaOH solution for 2 h at 80 ºC followed by bleaching process using a solution made up of 1.7 wt% aqueous sodium hypochlorite, acetate buffer (0.2 M, pH 4.8) and water (1:1:1) for 4 h at 80 ºC, in order to remove extractives, hemicellulose and lignin of the raw material. Subsequently, the bleached fibres were hydrolysed with sulfuric acid (65 wt%) for 45 min at 45 ºC. The excess acid was then removed from the solution by washing with Milli-Q water by repetitive centrifugation and finally by dialysis. The resulting suspension was sonicated to promote CNCs dispersion and then centrifuged to remove the remaining unhydrolyzed fibres. The collected suspension was then stored in a refrigerator for further use.

2.4 Preparation of reinforced protein films

Preparation of FBP films was done by solution casting process. Control protein films were prepared dissolving FBP (5% w/v), glycerol (50% w/w based on the dry weight of FBP) and distilled water. The pH of the solution was adjusted to 10.5 using a 1M NaOH solution and was mechanically stirred for 1 h. After this, the solution was denatured by heating at 85 ºC for 30 min in a water bath and cooled down at room temperature. For the CNCs-reinforced films, the same procedure was followed as for the control film, however in this case the appropriate amounts of CNCs were incorporated (1, 3, 5 and 7 wt% on the dry weight of FBP) after the denaturation process, keeping the solution in a stirrer for 30 minutes. The resulting solutions were casted into a polystyrene Petri dish and dried at 40 ºC for 24 h. Then, the dried films were peeled off and conditioned at 52% relative humidity (RH) and 25 °C for 48 h prior to testing. All films were prepared in triplicate. **Table 1** summarizes the composition of all the developed films.

Table 1. Composition and codes for faba beans proteins (FBP) films with different pine cone cellulose nanocrystals content.

Samples	Content			
	Proteins (g)	Glycerol (g)	Water (g)	CNC (wt% on dry proteins)
FBP	5	2.5	100	0
FBP_CNC-1	5	2.5	100	1
FBP_CNC-3	5	2.5	100	3
FBP_CNC-5	5	2.5	100	5
FBP_CNC-7	5	2.5	100	7

2.5 Characterization techniques

2.5.1 Film thickness

The thickness of the FBP films was determined at ten random points around each film sample using a manual micrometer Mitutoyo No. 2109S-10 (Tokyo, Japan) with 0.001 mm sensitivity. The average value of each film was determined and used in calculations for mechanical properties, oxygen transmission rate, water vapour transmission rate and transparency.

2.5.2 Mechanical properties

The mechanical tensile properties, namely the tensile strength (TS), the Young's modulus (E) and the elongation at break (ε) of FBP films were determined following the standard method ASTM D882-02, using a Linkam TST-350 tensile stage (Linkam Scientific Instruments, Ltd., U.K.) with a 20 N load cell. Preconditioned FBP films were cut into rectangular strips (30 x 4 mm^2) and placed between the tensile grips. The initial grip distance was set at 15 mm and the crosshead speed at 5 mm min^{-1}. At least five specimens from each film were tested at room temperature and the average results were obtained.

2.5.3 Thermogravimetric analysis (TGA)

Thermal behaviour of different FBP films obtained was analyzed by thermogravimetric analysis using a Mettler-Toledo TGA/DSC 1 thermobalance (Schwerzenbach, Switzerland). Samples with

a total weight between 8-10 mg were placed in an alumina crucible (70 µL) and heated from 30 to 800 ºC at a constant heating rate of 10 ºC min^{-1} under nitrogen atmosphere (flow rate 50 mL min^{-1}). All samples were analyzed in triplicate to ensure reproducibility.

2.5.4 Moisture content

Moisture content of FBP films samples was determined gravimetrically by measuring the weight loss of films, with a size of 1 x 1 cm^2, before and after drying in an oven at 105 ºC for 24 h, to attain a constant weight. The moisture content of each film was calculated according to the following Equation (1):

$$Moisture\ content\ (\%) = 100 \times \left[\frac{W_i - W_f}{W_i}\right] \quad \text{(Eq. 1)}$$

Where W_i and W_f are the initial and dried weight of the samples respectively. Three replications of each film were used for calculating the moisture content average.

2.5.5 Solubility

The solubility of FBP films in water was determined according to the method proposed by K. Masamba *et al.* (Masamba, et al., 2016) with minor modifications. Rectangular pieces of films (10 x 10 mm^2) were dried in an oven at 105 ºC for 24 h, until constant weight. The weight of the dried films was measured, and then the films were placed into a test tube with 10 mL of distilled water. The tubes were slowly and periodically stirred for 24 h at 25 ºC. After that period, the non-solubilized fraction was dried in the oven at 105 °C for 24 h in order to determine the weight of dry matter not dissolved in water. The % solubility of each film was determined using the following equation (2):

$$Solubility\ (\%) = 100 \times \left[\frac{W_i - W_f}{W_i}\right] \quad \text{(Eq. 2)}$$

Where W_i is the initial weight of the sample and W_f is the sample weight after drying. The measurements were made in triplicate.

2.5.6 Static contact angle measurements

The static contact angle (θ) of each preconditioned FBP films was measured by an optical goniometer model FM140 (110/220 V, 50/60 Hz) from KRÜSS GmbH (Hamburg, Germany) at room temperature. This goniometer is equipped with a video capture kit and analysis software (Drop Shape Analysis SW21; DSA1). Five different water droplets, using distilled water as contact liquid, were deposited onto the film surface with a micro syringe and ten measurements were obtained for each drop and averaged. The contact angle was measured 30 s after depositing the drop to obtain stabilized values.

2.5.7 Transparency

FBP films transparency was determined using a UV-Vis spectrophotometer Perkin Elmer model Lambda 2 (Massachusetts, EEUU) according to ASTM D1746. Preconditioned film specimens were cut into rectangle shape and directly placed in the spectrophotometer cell. The percent transmittance of light at 600 nm in each film was measured by triplicate, and the transparency value was calculated by the following equation (3):

$$Transparency = \left[\frac{LogT_{600}}{x}\right] \quad \text{(Eq. 3)}$$

Where T_{600} is the transmittance at 600 nm of each film and x is the film thickness (mm).

2.5.8 Colour of films

The effect of CNCs in the colour properties of FBP films was studied in a colorimeter model KONICA CM-3600d COLORFLEX-DIFF2 from Hunter Associates Laboratory (Virginia, EEUU) calibrated using a white standard. The CIELAB colour space was used to measure the

265 degree of L^* (lightness), a^* (red-green) and b^* (yellow-blue) of each film. Five measurements
266 were made at random positions over each film surface and average values were calculated. Total
267 colour difference (ΔE) was calculated using the following equation (4):
268
269 $$\Delta E = \sqrt{(\Delta L^*)^2 + (\Delta a^*)^2 + (\Delta b^*)^2} \quad \text{(Eq. 4)}$$
270
271 Where ΔL^*, Δa^* and Δb^* are the differences between the corresponding colour parameters of the
272 samples and the colour parameter values of the control film (L^* = 66.6, a^* = 5.5, b^* = 37.0).
273
274 *2.5.9 Oxygen Transmission Rate (OTR)*
275 The oxygen transmission rate (OTR) of the FBP films was obtained using an OTR Permeation
276 Analyzer Mocon OX-TRAN model 2/20 from Modern Controls Inc. (Minneapolis, USA)
277 equipped with a coulometric oxygen sensor in accordance with ASTM D3985-95. The area of
278 measurement of the samples was 5 cm^2 and the OTR measurements were performed at 23 ºC and
279 50% RH. Before the analysis, the samples were conditioned for 2 days at 23 ºC and 50% RH. At
280 least two samples of each film were tested.
281
282 *2.5.10 Water vapor permeability (WVP)*
283 The WVP test was conducted gravimetrically in triplicate following ASTM E96-95. Conditioned
284 circular films were sealed on permeability cups TQC Sheen B.V. model VF2200 (Capelle aan
285 den IJssel, Netherlands) containing 2 g of $CaCl_2$ (0% RH) with an exposed area of 10 cm^2. Later,
286 the cups were placed in a desiccator at 25 ± 1 °C containing a saturated $Mg(NO_3)\cdot 6H_2O$ solution
287 to reach a relative humidity of 54% ± 3%. The cups were weighed each hour for a total period of
288 8 hours using an analytical balance. The changes in cup weight were plotted as a function of time
289 and the slope was calculated by linear regression. Finally, the WVTR was calculated according
290 to the following equation (5) (Trifol, et al., 2016):
291

$$WVTR = \frac{n \times l}{S} \quad \text{(Eq. 5)}$$

Where *n* is the slope of the straight line, *l* is the thickness of the film and *S* is the exposed area of the film.

2.5.11 Field Emission Scanning Electron Microscopy (FESEM)

The morphology of the cross section of nitrogen cryofractured films was studied in a field emission scanning electron microscope (FESEM) ZEISS model ULTRA55 (Eindhoven, The Netherlands) with an operating voltage of 1 kV. Prior to the morphological characterization, the cryofracture surface of films were coated with a thin layer of platinum in a high vacuum sputter coater EM MED20 from Leica Microsystems (Milton Keynes, United Kingdom).

2.5.12 Attenuated total reflection-Fourier transform infrared (ATR-FTIR) spectroscopy

The FBP films spectra were recorded by attenuated total reflection method (ATR) in an infrared spectrometer Perkin-Elmer Spectrum BX (Perkin-Elmer Spain S.L., Madrid, Spain). Each sample was subjected to 20 scans between 4000 and 600 cm^{-1} with a resolution of 4 cm^{-1}. After attenuation of total reflectance and baseline correction, spectra were normalized with a limit ordinate of 1.5 absorbance units.

3. RESULTS AND DISCUSSION

3.1 Mechanical Properties

The mechanical properties of the control film (FBP) and films reinforced with different CNCs content are shown in Fig. 1. As can be seen, the incorporation of low CNCs content (1 and 3 wt%) to the FBP film hardly affects the strength and tensile modulus, obtaining values very similar to those of the unreinforced FBP film. However, it is observed that the addition of higher CNCs amounts (5 and 7 wt%) results in a considerable increase in tensile strength, with values of 5.3 MPa and 6.5 MPa for the films reinforced with 5 and 7 wt% of CNCs respectively, which

represents a percentage increase of 22.3% and 50.5% respectively, with respect to the unreinforced film (4.3 MPa). The tensile strength values obtained with the film reinforced with 7 wt% CNCs are higher than those obtained with other protein films reinforced with similar or higher amounts of CNCs (González, et al., 2015; Osorio-Ruiz, et al., 2019; Sukyai, et al., 2018). This tendency is also observed in Young's modulus, where it can be seen that the addition of 5 and 7 wt% of CNCs into the FBP film resulted in an increase of 43.7% and 76.1% respectively with respect to the unreinforced protein film (67.1 MPa). Therefore, the incorporation of CNCs into the FBP film resulted in an increase in its stiffness, which increases with the amount of reinforcement in the matrix. This is due to the increased hydrogen bonds formed between the protein matrix and the reinforcement as CNCs loading increases, thus increasing the cohesion of the films and reducing their flexibility (González, et al., 2015; Sukyai, et al., 2018). This same trend with respect to mechanical strength properties was observed by Sukyai *et al.* (Sukyai, et al., 2018) who studied the effect of different content of cellulose nanocrystals from sugarcane bagasse (0, 2, 5 and 8 wt%) in whey protein films. In this case, the authors observed that the addition of 8 wt% CNCs to the whey protein film resulted in an increase in tensile strength from 2.30 MPa to 4.93 MPa and Young's modulus from 57.56 MPa to 187.42MPa with respect to the unreinforced whey protein film.

With respect to the elongation at break, Fig. 1 shows how the addition of CNCs results in a decrease of ductile mechanical properties of the FBP film. In this case, it is observed that the control film shows an elongation at break of about 105%. This elongation at break is significantly higher than the elongation at break obtained in other protein films with similar plasticizer content, such as soy protein films (González, Gastelú, Barrera, Ribotta, & Igarzabal, 2019) or whey protein films (Galus & Kadzińska, 2016). The addition of 1 wt% of CNCs considerably reduces the elongation at break of the control film, changing from 104.4% in FBP film to 63.9%. For higher amounts of CNCs (3 and 5 wt%) the elongation at break decreases to around 54%, while for films reinforced with 7 wt% CNCs the elongation decreases to 48.9%, which represents a decrease of around 53.1% with respect to the elongation at break of the control film. This decrease in elongation at break is typical of protein films reinforced with cellulose nanocrystals, since the

interactions of the CNCs with the proteins lead to a reduction in the polymer chains' mobility, thus reducing their ductility (Shabanpour, Kazemi, Ojagh, & Pourashouri, 2018).

Comparing the mechanical properties of unreinforced FBP films and films reinforced with different CNCs content with those of synthetic films used in the food packaging sector, it can be observed that the elongation at break obtained in the control film is higher than that of widely used materials such as PET (70%) or HDPE (20-50%). However, these materials have higher tensile strength values than FBP films. On the other hand, it is observed that the tensile strength achieved by the FBP film reinforced with 7 wt% CNCs has a tensile strength value similar to that of LDPE (7-25 MPa) and EVA (6-19 MPa) (Bastarrachea, Dhawan, & Sablani, 2011).

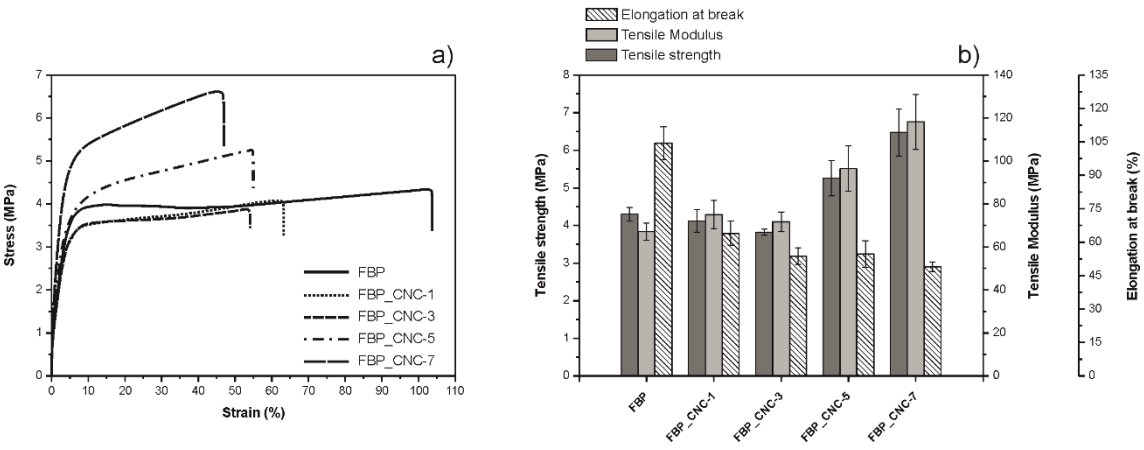

Fig. 1.- Tensile properties of unreinforced (control) FBP film and FBP film reinforced with different CNCs content: a) stress-strain curves and b) tensile properties.

3.2 Thermal properties

The thermal stability of unreinforced FBP film and films reinforced with different CNCs content was studied by thermogravimetric analysis. Fig. 2 shows the mass loss curves of the FBP films with respect to temperature and their corresponding first derivative curves (DTG). Additionally, Table 2 gathers the most relevant thermal degradation properties, namely the onset degradation temperature of each film and the maximum degradation temperatures in each of the different degradation stages, as well as the percentage of mass loss obtained in each of them. As can be

seen in all the curves, three main stages can be identified. The weight loss that occurs at low temperatures (30-125°C) is related to the moisture loss absorbed by the films. The second degradation stage (125-280°C) is attributed to the loss of low molecular weight protein fractions and glycerol evaporation. Finally, the third stage (280-500ºC), is related to the protein and CNCs degradation (Osorio-Ruiz, et al., 2019). As shown in Table 2, the control film (FBP) has a higher moisture content than the CNCs-reinforced films. This is a clear evidence of the increased hydrophobicity of the film due to the presence of the CNCs, as their interaction with the proteins reduces the number of active sites capable of reacting with the water molecules, thus reducing the moisture content of the film. It can also be observed that the FBP film onset degradation temperature increases with the presence of CNCs, with higher values as the CNCs content increases. In this case, the highest onset degradation temperature is obtained for the film reinforced with 7 wt% CNCs, with an increase of about 15 ºC with respect to the control film. On the other hand, if the third degradation stage is observed, related to the degradation of the proteins and CNCs, it can be seen that the reinforced films present higher thermal stability with increasing CNCs content. This increase in degradation temperature in reinforced films may be due to the higher thermal stability of CNCs compared to proteins, as well as the formation of strong intermolecular bonds between CNCs and the matrix phase resulting in improved thermal stability compared to the control film (Chang, Jian, Zheng, Yu, & Ma, 2010; Osorio-Ruiz, et al., 2019). In this case, the highest degradation temperature (T_{max3}) was obtained in the film reinforced with 7 wt% of CNCs, with a value of 318.9 ºC. This is due to the higher number of interactions established between the proteins and CNCs, resulting in an increase in their thermal stability.

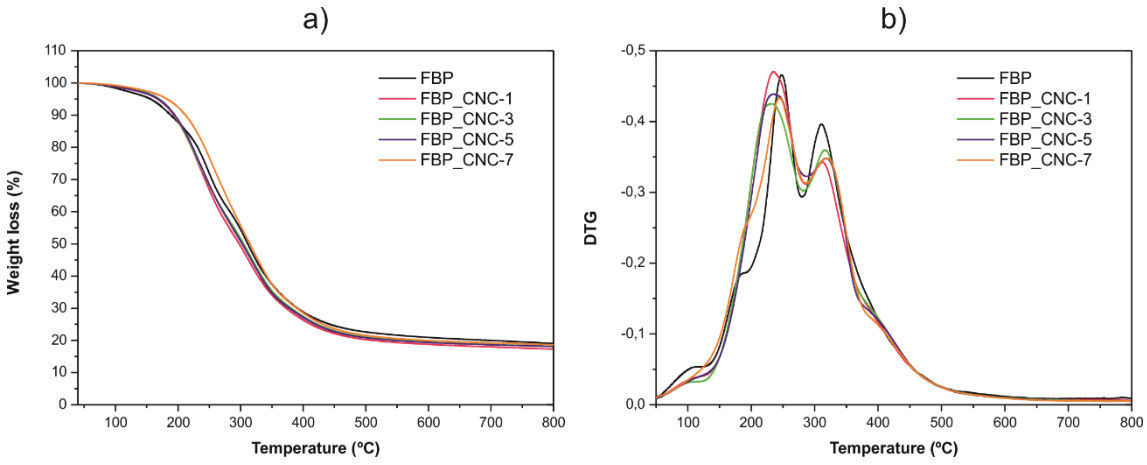

Fig. 2. a) TGA curves and b) DTGA curves of unreinforced (control) FBP film and FBP film reinforced with different CNCs content.

Table 2. Thermal parameters of unreinforced (control) FBP film and FBP film reinforced with different CNCs content.

Samples	T_0[a] (ºC)	Stage 1 30 - 125 ºC	Stage 2 125-280 ºC		Stage 3 280-500 ºC		Residue Mass (%)
		Mass loss (%)	Mass loss (%)	T_{max2} (ºC)	Mass loss (%)	T_{max3} (ºC)	
FBP	155.9 ± 0.1	2.8 ± 0.2	34.2 ± 2.9	245.9 ± 1.2	44.1 ± 3.3	311.9 ± 1.5	18.9 ± 0.3
FBP_CNC-1	165.4 ± 1.9	2.1 ± 0.0	45.6 ± 1.6	237.9 ± 1.7	35.3 ± 1.3	311.7 ± 0.7	17.1 ± 0.3
FBP_CNC-3	166.7 ± 1.4	2.0 ± 0.1	39.6 ± 1.6	235.0 ± 2.7	40.0 ± 1.2	316.4 ± 0.4	18.4 ± 0.3
FBP_CNC-5	167.1 ± 1.0	2.1 ± 0.0	43.7 ± 1.2	232.8 ± 1.9	36.3 ± 0.9	318.5 ± 0.5	17.9 ± 0.3
FBP_CNC-7	170.8 ± 2.1	1.9 ± 0.2	43.2 ± 3.4	243.7 ± 3.7	36.3 ± 3.0	318.9 ± 0.6	18.6 ± 0.1

[a] T_0 is calculated at 5% weight loss.

3.3 Water susceptibility

Moisture content, water solubility and contact angle values of different FBP films are shown in Table 3. As can be seen, the addition of CNCs to the protein film results in a slight reduction in the moisture content of the films, being this reduction greater for higher CNCs contents (5 and 7%). This decrease in the moisture content of the reinforced films may be due to the interactions formed between the hydroxyl groups of the CNCs and the free functional groups of the proteins, which reduce the number of available active sites capable of interacting with the water molecules, resulting in an increase in the hydrophobicity (Qazanfarzadeh, et al., 2016). This reduction of hydrophilic groups in the protein film due to interactions with CNCs also leads to an increase in the surface hydrophobicity. As can be seen in Table 3, the contact angle of the control film (56.7º) increases after the addition of CNCs, being higher as the CNCs concentration in the film increases. In this case, the maximum contact angle is obtained for the FBP film reinforced with 7 wt% CNCs, with a contact angle of 66.7º, which represents an increase of 21.4% with respect to the control film (Condés, et al., 2015). This increase in FBP film hydrophobicity after CNCs incorporation is of great interest for food packaging applications. However, the contact angle is

still lower than that of materials used as food packaging such as LDPE (100.2°), HDPE (92.4°) or PP (90°), which is evidence of their hydrophilic nature (Fávaro, Rubira, Muniz, & Radovanovic, 2007; Karbowiak, Debeaufort, Champion, & Voilley, 2006).

Table 3 shows the water solubility values of the different films. Water solubility is an important property to be considered in food packaging applications where the film has to be in contact with food that contains a large amount of water. In this case it is observed that the unreinforced FBP film shows a low water solubility compared to other protein films, such as soy protein films (González, et al., 2019; González, et al., 2015), whey protein (Sukyai, et al., 2018) or Amaranth protein films (Condés, et al., 2015). This low solubility of the films was evidenced by the good structural integrity obtained after 24 hours of immersion in water, which showed that only small amounts of low molecular weight peptides and plasticizer were dissolved in the water during the test (Wang, et al., 2017). In this case, it is observed that the incorporation of CNCs in the FBP film decreases its water solubility, obtaining a reduction in solubility of around 10% for films with CNCs contents of 3, 5 and 7 wt% compared to the control film. This reduction in solubility is due to the strong hydrogen bonding interactions established between the hydroxyl groups of CNCs and the carboxyl and amino groups of proteins, which improve their cohesion and reduce their susceptibility to water molecules (Abdollahi, Alboofetileh, Behrooz, Rezaei, & Miraki, 2013; Shabanpour, et al., 2018). Some authors have reported that this reduction in water solubility may also be influenced by the high crystallinity of the CNCs (Deepa, et al., 2016).

Table 3. Moisture content, water solubility and contact angle for unreinforced (control) FBP film and FBP film reinforced with different CNCs content.

Samples	Sample				
	FBP	**FBP_CNC-1**	**FBP_CNC-3**	**FBP_CNC-5**	**FBP_CNC-7**
Moisture content (%)	15.9 ± 0.5	15.4 ± 0.6	15.3 ± 0.7	14.2 ± 0.3	14.3 ± 0.9
Water solubility (%)	34.6 ± 0.5	33.6 ± 0.2	31.7 ± 0.5	31.1 ± 1.1	31.5 ± 0.8
Contact angle (º)	56.7 ± 1.3	57.4 ± 2.1	61.6 ± 1.4	64.6 ± 3.1	66.7 ± 1.0

436 **3.4 Chemical structural properties**

437 The chemical interactions between CNCs and the proteins during film production were assessed
438 by ATR-FTIR. Fig. 3 shows the FTIR spectra of the unreinforced FBP film and the films
439 reinforced with different CNCs content. As can be seen, the control film spectra (FBP) shows the
440 main absorption bands of the peptide linkage which are the peak at 1630 cm^{-1} corresponding to
441 the amide I band (C═O stretching), the peak at 1538 cm^{-1} attributed to the amide II band (N−H
442 bending and C−N stretching) and the peak at 1238 cm^{-1} corresponding to the amide III band (N−H
443 bending and C−N stretching) (Montalvo-Paquini, et al., 2014). Other characteristic peaks
444 appearing in the spectra are the peak at 3272 cm^{-1} related to the N−H and O−H groups of the
445 proteins, and the peak at 1038 cm^{-1} associated with C−C and C−O stretching vibrations. On the
446 other hand, the peaks located in the range between 800 and 1150 cm^{-1} are attributed to the glycerol
447 used as a film plasticizer (Shabanpour, et al., 2018; Sogut, 2020; Sukyai, et al., 2018). After the
448 incorporation of CNCs, no significant changes in the spectra were observed. However, it is
449 observed that in the reinforced films a new peak appears at 1158 cm^{-1} related to the saccharide
450 structures of CNCs (Yu, et al., 2018), as well as a change in the intensity of the bands associated
451 to the amide I, II, and III compared to the control film. These differences are most evident in the
452 case of the film reinforced with 7 wt% CNCs. This suggests the formation of interactions between
453 the main polypeptide chains of proteins and the CNCs, consisting mainly of hydrogen bonds
454 between the amino and carboxyl groups of the proteins and the hydroxyl groups of the CNCs
455 (Martelli-Tosi, et al., 2018; Shabanpour, et al., 2018).

456

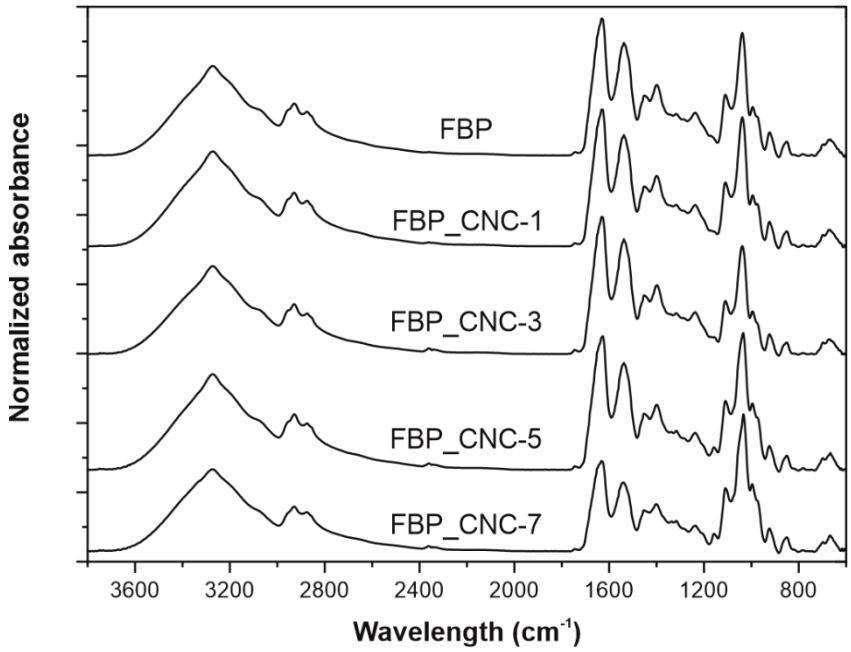

Fig. 3. FTIR spectra of unreinforced (control) FBP film and FBP film reinforced with different CNCs content.

3.5 Morphological properties

The FESEM images of the cryofractured cross section of the different films are gathered in Fig. 4. As can be seen, the control film has a smooth and homogeneous surface, with the presence of small microcracks and numerous surface pores. After the CNCs incorporation, a modification of the fracture surface is observed. In this case, CNCs-reinforced films have a higher cross-section roughness, which increases as the CNCs content in the film increases. Furthermore, it is observed that the CNCs incorporation in the film leads to a reduction in the size and pore number on the surface, resulting in a more homogeneous and uniform surface. This is most noticeable in samples reinforced with small CNCs content (1% and 3%). This reduction in the size and number of pores on the surface evidences the good interaction between the functional groups of the proteins, the glycerol and the CNCs, which results in more compact and resistant films, but with a lower molecular mobility, which is reflected in the mechanical properties with an increase in the tensile strength and a decrease in the elongation at break (Mirpoor, et al., 2020; Osorio-Ruiz, et al., 2019; Yu, et al., 2018).

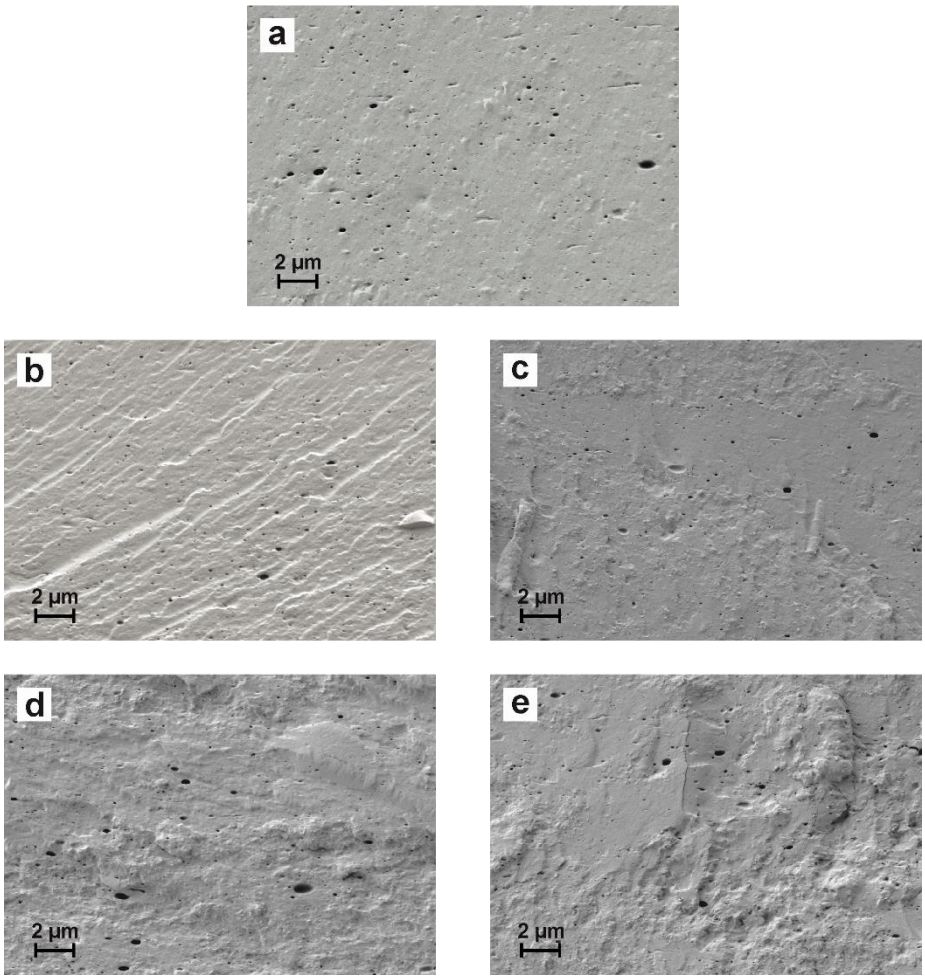

Fig. 4. Field emission scanning electron microscopy (FESEM) images at 5000× of cryofractured cross section of FBP-based films: (a) FBP (control); (b) FBP_CNC-1; (c) FBP_CNC-3; (d) FBP_CNC-5 and (e) FBP_CNC-7.

3.6 Barrier properties

Fig. 5 shows the OTR and WVTR values of unreinforced FBP film (control), and films reinforced with different CNCs content. As can be seen in Fig. 5a, the CNCs addition to the control FBP film results in a reduction of the OTR values, being this reduction greater as the CNCs content in the film increases. In this case, the lowest OTR value was obtained in the film with a CNCs content of 7 wt% (3.67×10^3 mL µm m^{-2} day^{-1}), obtaining an OTR value 36.2% lower than the control film (5.75×10^3 mL µm m^{-2} day^{-1}). This OTR decrease is due to the formation of a dense network structure by the interaction between proteins and CNCs which results in an increase in the tortuosity of the diffusion pathway of the oxygen molecules, hindering their transfer through

the film and thus increasing its oxygen barrier property (Xie, et al., 2020). This reduction of oxygen permeability is of great importance in the food packaging sector, as it allows to increase the product's shelf life.

In the same way, it can be seen in Fig. 5b that the WVTR is also reduced by the presence of CNCs, improving the water barrier property of the FBP films. In this case, the addition of 1 wt% CNCs hardly affects the water vapour permeability. However, higher CNCs content results in a decrease in WVTR with respect to the control film, leading to a greater decrease as the CNC content in the film increases. The WVTR of the control film was 2.93×10^4 g µm m^{-2} day^{-1}, reducing to 2.27×10^4 g µm m^{-2} day^{-1} after incorporating 7 wt% CNCs, a decrease of about 22.7%. This improvement of the water vapour barrier property of the reinforced films can be influenced by several aspects, such as the decrease of the films' hydrophilicity due to the presence of CNCs, or the increase of the tortuosity of the diffusion path of water molecules due to the presence of highly crystalline CNCs. In addition, the restricted polymer chain mobility and the higher matrix structure density obtained due to the strong interactions of the functional groups of proteins and CNCs also contribute to the reduction of the water vapour permeability of CNC-reinforced films. (Azevedo, et al., 2020; Rafieian, Shahedi, Keramat, & Simonsen, 2014).

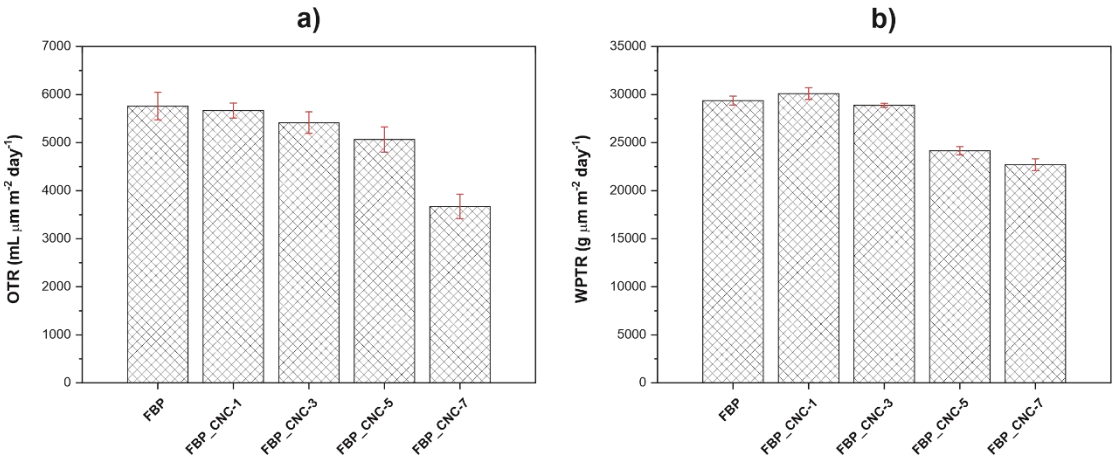

Fig. 5. a) OTR and b) WVTR of unreinforcing (control) FBP film and FBP film reinforcing with different CNCs content.

3.7 Colour and transparency properties

Fig. 6 shows the light transmission in the UV and visible ranges and the transparency of unreinforced FBP film and films reinforced with different CNCs content. As can be seen, all films show a good ability to absorb UV light at wavelengths between 250 and 300 nm, while for wavelengths between 300 and 400 nm, the CNCs addition to the FBP film reduces the UV light absorption, which is of interest in the food preservation packaging sector. In the visible range region (400-700 nm), the FBP film shows a high transmittance percentage, which is reduced after the CNCs incorporation. As can be seen in Fig. 6a, the transmittance decreases as the CNC content of the film increases.

The films' transparency is one of the most important properties to be considered for their use in the food packaging industry. Fig. 6b shows that the control film has a high transparency, however, after CNCs addition, this transparency is slightly reduced, obtaining a higher opacity as the CNCs content in the film increases. The decrease in transparency of the reinforced films may be related to light scattering caused by the dispersed CNCs in the matrix which leads to a reduction of light passing through the film. The increased opacity of reinforced films may also be due to the formation of CNCs aggregates during film fabrication, which cause a slight darkening and make it difficult for light to pass through the matrix (Qazanfarzadeh, et al., 2016; Shabanpour, et al., 2018). This loss of transparency in CNCs-reinforced protein films has also been observed by several authors such a Sukya *et al.* (Sukyai, et al., 2018), Han *et al*. (Han, et al., 2018) or Huang *et al.* (Huang, Tao, Ismail, & Wang, 2020). In this case, FBP films are less transparent than other CNCs-reinforced films, such as CNCs-reinforced whey protein films from sugar cane bagasse. (Sukyai, et al., 2018). However, it is worth noting that the control film and the FBP film reinforced with 1 wt% of CNCs show higher transparency than the commercial LDPE film used for food packaging, 4.26 A/mm, being this very similar to that obtained in the FBP films reinforced with 3, 5 and 7 wt% of CNCs (Guerrero, Hanani, Kerry, & De La Caba, 2011).

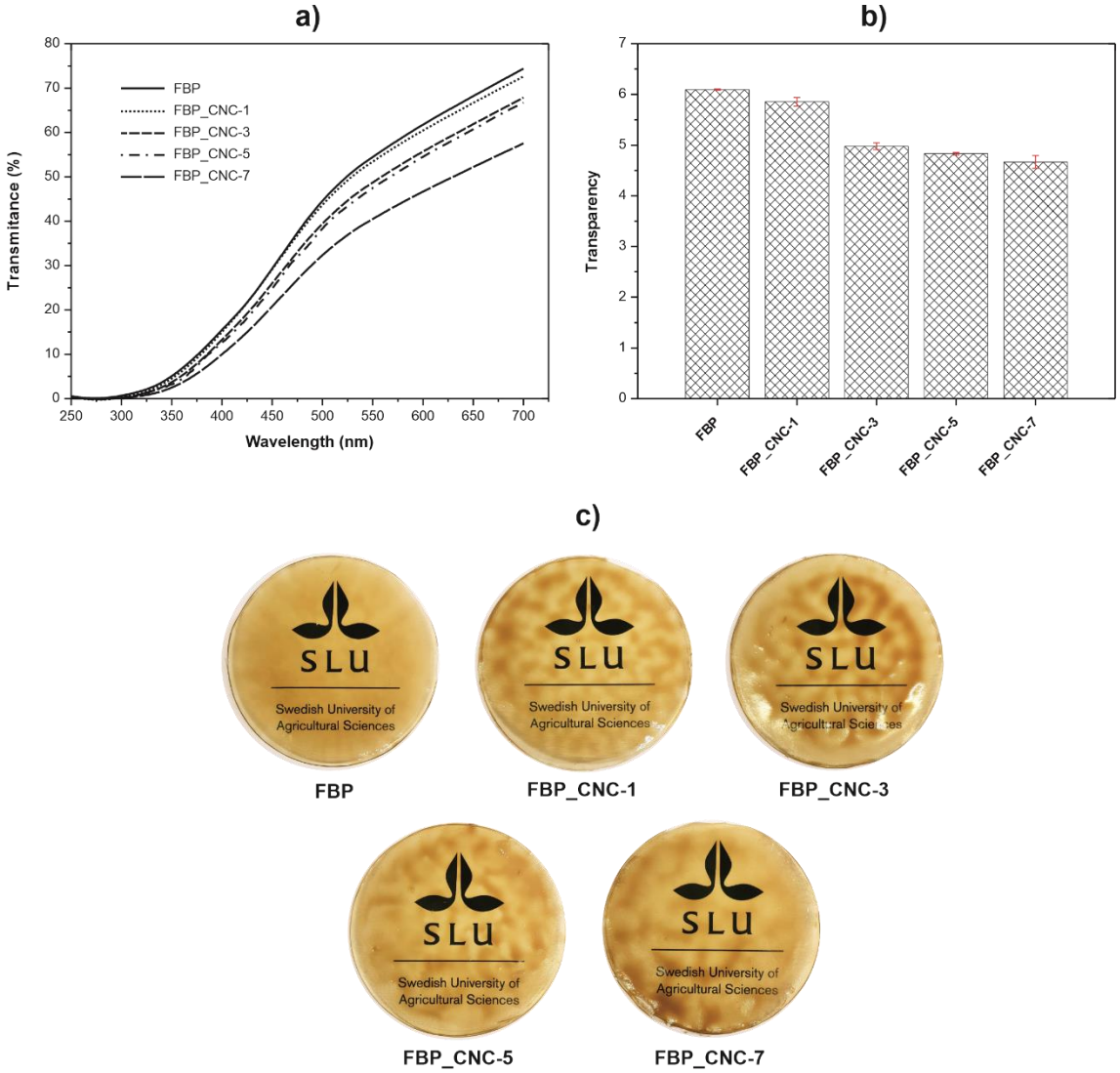

Fig. 6. a) transmittance, b) transparency and c) macroscopic aspect of unreinforced (control) FBP film and FBP film reinforced with different CNCs content.

Table 4 shows the surface colour values of unreinforced film and films reinforced with different CNCs content. As can be seen, the incorporation of CNCs into the FBP films results in a slight increase in L^* and a decrease in the a^* and b^* coordinate values, which is representative for a slight increase of the brown colour in the samples, probably due to the formation of CNC aggregates in the film. However, the ΔE values of the CNC-reinforced films show that the reinforcement addition into the FBP film hardly alters its colour properties.

548 **Table 4.** Colour parameters from CIELab space of unreinforced (control) FBP films and FBP
549 film reinforced with different CNCs content.

Parameter	FBP	FBP_CNC-1	FBP_CNC-3	FBP_CNC-5	FBP_CNC-7
*L**	66.6 ± 0.4	68.0 ± 0.7	69.8 ± 1.3	68.6 ± 1.6	69.4 ± 1.4
*a**	5.5 ± 0.3	4.3 ± 0.3	3.9 ± 0.6	5.1 ± 0.7	4.0 ± 0.5
*b**	37.0 ± 0.5	34.5 ± 0.8	35.6 ± 1.2	35.1 ± 1.3	34.2 ± 1.2
ΔE *(Control)*[a]	-	3.1	3.8	2.7	4.2

550 [a] ΔE is calculated from the color difference between FBP film and each FBP/CNC film.

551

552 **4. CONCLUSIONS**

553 In the present work, the effect of the incorporation of different CNCs content (1, 3, 5 and 7 wt%)
554 synthesized from pine cone on the mechanical, thermal, barrier, water susceptibility, optical and
555 morphological properties of faba bean protein (FBP) films has been evaluated. The CNCs addition
556 to the FBP film resulted in the formation of intramolecular interactions between the hydroxyl
557 groups of the CNCs and the amino and carboxyl groups of the proteins, mainly through hydrogen
558 bonds. This chemical affinity resulted in more compact films with lower chain mobility, which
559 was reflected in the mechanical properties of the reinforced films through an increase in tensile
560 strength and Young's modulus and a decrease in the elongation at break compared to the
561 unreinforced FBP film. In this case, the incorporation of 7 wt% CNC in the FBP film resulted in
562 an increase in tensile strength and Young's modulus of 50.5 and 76.1% respectively with respect
563 to the control film, as well as a decrease in elongation at break of about 53.1%. The thermal
564 stability of the FBP film was also affected by the presence of CNCs, increasing the onset
565 degradation temperature as the CNC content in the film increases. In this case, an increase of 15
566 ºC was obtained in the onset degradation temperature of the film reinforced with 7 wt% of CNCs
567 compared to the control film. A slight increase in the maximum degradation temperature was also
568 observed in the reinforced films with respect to the FBP film. The interactions formed between
569 the CNCs and the proteins also reduced the amount of active sites able to react with the water
570 molecules in the proteins, which resulted in an increase in the hydrophobicity of the CNC-
571 reinforced films, as evidenced by a reduction in moisture content and water solubility and an

increase in their contact angles. The CNCs addition to the FBP film also significantly improved its barrier properties, reducing its WVTR and OTR as the CNC content in the matrix increased. In this case, the film reinforced with 7 wt% CNC obtained 36.2 and 22.7% lower OTR and WVTR values, respectively, compared to the unreinforced FBP film. Finally, it was observed that the presence of CNCs in the FBP film led to an increase in its opacity as the CNCs content increases. This work has shown that CNCs obtained from pine cone are of great interest to improve some physical and mechanical properties of FBP films, obtaining biobased and biodegradable materials that could present attracting potential for use in the food packaging sector as edible food packaging material. These films could be a potential solution to reduce the amount of non-degradable food packaging waste of petrochemical origin.

Acknowledgements

This research was supported by the Ministry of Science and Innovation (MICI) [MAT2017-84909-C2-2-R]. S. Rojas-Lema thanks the Generalitat Valenciana (GVA) for the financial support through a Santiago Grisolia grant (GRISOLIAP/2019/132). D. Garcia-Garcia wants to thank the Ministry of Science, Innovation and Universities for their financial support through the "José Castillejo" mobility grant (CAS19/00332).

590 **References**

591 Abdollahi, M., Alboofetileh, M., Behrooz, R., Rezaei, M., & Miraki, R. (2013). Reducing
592 water sensitivity of alginate bio-nanocomposite film using cellulose nanoparticles.
593 *International journal of biological macromolecules, 54*, 166-173.

594 Aguirre, A., Borneo, R., & León, A. E. (2013). Properties of triticale protein films and their
595 relation to plasticizing–antiplasticizing effects of glycerol and sorbitol. *Industrial Crops*
596 *and Products, 50*, 297-303.

597 Azevedo, V. M., de Oliveira, A. C. S., Borges, S. V., Raguzzoni, J. C., Dias, M. V., & Costa,
598 A. L. R. (2020). Pea protein isolate nanocomposite films for packaging applications:
599 Effect of starch nanocrystals on the structural, morphological, thermal, mechanical and
600 barrier properties. *Emirates Journal of Food and Agriculture, 32*(7), 495-504.

601 Azevedo, V. M., Dias, M. V., de Siqueira Elias, H. H., Fukushima, K. L., Silva, E. K.,
602 Carneiro, J. d. D. S., Soares, N. d. F. F., & Borges, S. V. (2018). Effect of whey protein
603 isolate films incorporated with montmorillonite and citric acid on the preservation of
604 fresh-cut apples. *Food Research International, 107*, 306-313.

605 Azevedo, V. M., Silva, E. K., Pereira, C. F. G., da Costa, J. M. G., & Borges, S. V. (2015).
606 Whey protein isolate biodegradable films: Influence of the citric acid and montmorillonite
607 clay nanoparticles on the physical properties. *Food Hydrocolloids, 43*, 252-258.

608 Bastarrachea, L., Dhawan, S., & Sablani, S. S. (2011). Engineering properties of polymeric-
609 based antimicrobial films for food packaging: a review. *Food Engineering Reviews, 3*(2),
610 79-93.

611 Bourtoom, T. (2009). Edible protein films: properties enhancement. *International Food*
612 *Research Journal, 16*(1), 1-9.

613 Calva-Estrada, S. J., Jiménez-Fernández, M., & Lugo-Cervantes, E. (2019). Protein-based
614 films: Advances in the development of biomaterials applicable to food packaging. *Food*
615 *Engineering Reviews, 11*(2), 78-92.

Chang, P. R., Jian, R., Zheng, P., Yu, J., & Ma, X. (2010). Preparation and properties of glycerol plasticized-starch (GPS)/cellulose nanoparticle (CN) composites. *Carbohydrate polymers, 79*(2), 301-305.

Condés, M. C., Añón, M. C., Mauri, A. N., & Dufresne, A. (2015). Amaranth protein films reinforced with maize starch nanocrystals. *Food Hydrocolloids, 47*, 146-157.

Deepa, B., Abraham, E., Pothan, L. A., Cordeiro, N., Faria, M., & Thomas, S. (2016). Biodegradable nanocomposite films based on sodium alginate and cellulose nanofibrils. *Materials, 9*(1), 50.

Fathi, N., Almasi, H., & Pirouzifard, M. K. (2019). Sesame protein isolate based bionanocomposite films incorporated with TiO2 nanoparticles: Study on morphological, physical and photocatalytic properties. *Polymer Testing, 77*, 105919.

Fávaro, S., Rubira, A., Muniz, E., & Radovanovic, E. (2007). Surface modification of HDPE, PP, and PET films with KMnO4/HCl solutions. *Polymer Degradation and Stability*, *92*(7), 1219-1226.

Galus, S., & Kadzińska, J. (2016). Whey protein edible films modified with almond and walnut oils. *Food Hydrocolloids, 52*, 78-86.

García-García, D., Balart, R., Lopez-Martinez, J., Ek, M., & Moriana, R. (2018). Optimizing the yield and physico-chemical properties of pine cone cellulose nanocrystals by different hydrolysis time. *Cellulose, 25*(5), 2925-2938.

Garcia-Garcia, D., Lopez-Martinez, J., Balart, R., Strömberg, E., & Moriana, R. (2018). Reinforcing capability of cellulose nanocrystals obtained from pine cones in a biodegradable poly (3-hydroxybutyrate)/poly (ε-caprolactone)(PHB/PCL) thermoplastic blend. *European Polymer Journal, 104*, 10-18.

González, A., Gastelú, G., Barrera, G. N., Ribotta, P. D., & Igarzabal, C. I. Á. (2019). Preparation and characterization of soy protein films reinforced with cellulose nanofibers obtained from soybean by-products. *Food Hydrocolloids, 89*, 758-764.

González, A., & Igarzabal, C. I. A. (2015). Nanocrystal-reinforced soy protein films and their application as active packaging. *Food Hydrocolloids, 43*, 777-784.

Guerrero, P., Hanani, Z. N., Kerry, J., & De La Caba, K. (2011). Characterization of soy protein-based films prepared with acids and oils by compression. *Journal of Food Engineering, 107*(1), 41-49.

Han, Y., Yu, M., & Wang, L. (2018). Soy protein isolate nanocomposites reinforced with nanocellulose isolated from licorice residue: Water sensitivity and mechanical strength. *Industrial Crops and Products, 117*, 252-259.

Hopkins, E. J., Stone, A. K., Wang, J., Korber, D. R., & Nickerson, M. T. (2019). Effect of glycerol on the physicochemical properties of films based on legume protein concentrates: A comparative study. *Journal of texture studies, 50*(6), 539-546.

Huang, S., Tao, R., Ismail, A., & Wang, Y. (2020). Cellulose Nanocrystals Derived from Textile Waste through Acid Hydrolysis and Oxidation as Reinforcing Agent of Soy Protein Film. *Polymers, 12*(4), 958.

Kang, H., Liu, X., Zhang, S., & Li, J. (2017). Functionalization of halloysite nanotubes (HNTs) via mussel-inspired surface modification and silane grafting for HNTs/soy protein isolate nanocomposite film preparation. *Rsc Advances, 7*(39), 24140-24148.

Karbowiak, T., Debeaufort, F., Champion, D., & Voilley, A. (2006). Wetting properties at the surface of iota-carrageenan-based edible films. *Journal of colloid interface science, 294*(2), 400-410.

Kumar, P., Sandeep, K., Alavi, S., Truong, V., & Gorga, R. (2010). Preparation and characterization of bio-nanocomposite films based on soy protein isolate and montmorillonite using melt extrusion. *Journal of Food Engineering, 100*(3), 480-489.

Langton, M., Ehsanzamir, S., Karkehabadi, S., Feng, X., Johansson, M., & Johansson, D. P. (2020). Gelation of faba bean proteins-Effect of extraction method, pH and NaCl. *Food Hydrocolloids, 103*, 105622.

668 Li, Y., Jiang, Y., Liu, F., Ren, F., Zhao, G., & Leng, X. (2011). Fabrication and
669 characterization of TiO2/whey protein isolate nanocomposite film. *Food Hydrocolloids*,
670 *25*(5), 1098-1104.

671 Liminana, P., Garcia-Sanoguera, D., Quiles-Carrillo, L., Balart, R., & Montanes, N. (2018).
672 Development and characterization of environmentally friendly composites from poly
673 (butylene succinate)(PBS) and almond shell flour with different compatibilizers.
674 *Composites Part B: Engineering*, *144*, 153-162.

675 Liu, X., Kang, H., Wang, Z., Zhang, W., Li, J., & Zhang, S. (2017). Simultaneously
676 toughening and strengthening soy protein isolate-based composites via
677 carboxymethylated chitosan and halloysite nanotube hybridization. *Materials*, *10*(6), 653.

678 Liu, Y., Xu, L., Li, R., Zhang, H., Cao, W., Li, T., & Zhang, Y. (2019). Preparation and
679 characterization of soy protein isolate films incorporating modified nano-TiO2.
680 *International Journal of Food Engineering*, *15*(7).

681 Makri, E., Papalamprou, E., & Doxastakis, G. (2005). Study of functional properties of seed
682 storage proteins from indigenous European legume crops (lupin, pea, broad bean) in
683 admixture with polysaccharides. *Food Hydrocolloids*, *19*(3), 583-594.

684 Martelli-Tosi, M., Masson, M. M., Silva, N. C., Esposto, B. S., Barros, T. T., Assis, O. B., &
685 Tapia-Blácido, D. R. (2018). Soybean straw nanocellulose produced by enzymatic or acid
686 treatment as a reinforcing filler in soy protein isolate films. *Carbohydrate polymers*, *198*,
687 61-68.

688 Masamba, K., Li, Y., Hategekimana, J., Liu, F., Ma, J., & Zhong, F. (2016). Effect of Gallic
689 acid on mechanical and water barrier properties of zein-oleic acid composite films.
690 *Journal of food science and technology*, *53*(5), 2227-2235.

691 Mirpoor, S. F., Giosafatto, C. V. L., Di Pierro, P., Di Girolamo, R., Regalado-González, C.,
692 & Porta, R. (2020). Valorisation of Posidonia oceanica Sea Balls (Egagropili) as a

693 Potential Source of Reinforcement Agents in Protein-Based Biocomposites. *Polymers*,
694 *12*(12), 2788.

695 Montalvo-Paquini, C., Rangel-Marrón, M., Palou, E., & López-Malo, A. (2014). Physical and
696 chemical properties of edible films from faba bean protein. *Cellulose, 8*, 125-131.

697 Moriana, R., Vilaplana, F., & Ek, M. (2016). Cellulose nanocrystals from forest residues as
698 reinforcing agents for composites: A study from macro-to nano-dimensions.
699 *Carbohydrate polymers, 139*, 139-149.

700 Nivala, O., Nordlund, E., Kruus, K., & Ercili-Cura, D. (2020). The effect of heat and
701 transglutaminase treatment on emulsifying and gelling properties of faba bean protein
702 isolate. *LWT - Food Science and Technology*, 110517.

703 Osorio-Ruiz, A., Avena-Bustillos, R. J., Chiou, B.-S., Rodríguez-González, F., & Martinez-
704 Ayala, A.-L. (2019). Mechanical and Thermal Behavior of Canola Protein Isolate Films
705 As Improved by Cellulose Nanocrystals. *ACS omega, 4*(21), 19172-19176.

706 Pereira, R. C., Carneiro, J. d. D. S., Assis, O. B., & Borges, S. V. (2017). Mechanical and
707 structural characterization of whey protein concentrate/montmorillonite/lycopene films.
708 *Journal of the Science of Food and Agriculture, 97*(14), 4978-4986.

709 Pérez, L. M., Piccirilli, G. N., Delorenzi, N. J., & Verdini, R. A. (2016). Effect of different
710 combinations of glycerol and/or trehalose on physical and structural properties of whey
711 protein concentrate-based edible films. *Food Hydrocolloids, 56*, 352-359.

712 Plastics Europe. (2020). *An analysis of European plastics production, demand and waste*
713 *data*. Retrieved from https://www.plasticseurope.org/en/resources/market-data.
714 Accessed July 5, 2021

715 Qazanfarzadeh, Z., & Kadivar, M. (2016). Properties of whey protein isolate nanocomposite
716 films reinforced with nanocellulose isolated from oat husk. *International journal of*
717 *biological macromolecules, 91*, 1134-1140.

718 Rafieian, F., Shahedi, M., Keramat, J., & Simonsen, J. (2014). Mechanical, thermal and
719 barrier properties of nano-biocomposite based on gluten and carboxylated cellulose
720 nanocrystals. *Industrial Crops and Products, 53*, 282-288.

721 Ramos, Ó. L., Reinas, I., Silva, S. I., Fernandes, J. C., Cerqueira, M. A., Pereira, R. N.,
722 Vicente, A. A., Pocas, M. F., Pintado, M. E., & Malcata, F. X. (2013). Effect of whey
723 protein purity and glycerol content upon physical properties of edible films manufactured
724 therefrom. *Food Hydrocolloids, 30*(1), 110-122.

725 Reddy, N., Jiang, Q., & Yang, Y. (2012). Preparation and properties of peanut protein films
726 crosslinked with citric acid. *Industrial Crops and Products, 39*, 26-30.

727 Rosa, D., Bardi, M., Machado, L., Dias, D., Silva, L., & Kodama, Y. (2010). Starch
728 plasticized with glycerol from biodiesel and polypropylene blends: mechanical and
729 thermal properties. *Journal of Thermal Analysis Calorimetry, 102*(1), 181-186.

730 Salgado, P. R., Ortiz, S. E. M., Petruccelli, S., & Mauri, A. N. (2010). Biodegradable
731 sunflower protein films naturally activated with antioxidant compounds. *Food*
732 *Hydrocolloids, 24*(5), 525-533.

733 Samaei, S. P., Ghorbani, M., Tagliazucchi, D., Martini, S., Gotti, R., Themelis, T., Tesini, F.,
734 Gianotti, A., Toschi, T. G., & Babini, E. (2020). Functional, nutritional, antioxidant,
735 sensory properties and comparative peptidomic profile of faba bean (Vicia faba, L.) seed
736 protein hydrolysates and fortified apple juice. *Food Chemistry, 330*, 127120.

737 Saremnezhad, S., Azizi, M., Barzegar, M., Abbasi, S., & Ahmadi, E. (2011). Properties of a
738 new edible film made of faba bean protein isolate. *Journal of Agricultural Science and*
739 *Technology, 13*(2), 181-192.

740 Shabanpour, B., Kazemi, M., Ojagh, S. M., & Pourashouri, P. (2018). Bacterial cellulose
741 nanofibers as reinforce in edible fish myofibrillar protein nanocomposite films.
742 *International journal of biological macromolecules, 117*, 742-751.

743 Silvério, H. A., Neto, W. P. F., Dantas, N. O., & Pasquini, D. (2013). Extraction and
744 characterization of cellulose nanocrystals from corncob for application as reinforcing
745 agent in nanocomposites. *Industrial Crops and Products, 44*, 427-436.

746 Slavutsky, A. M., & Bertuzzi, M. A. (2014). Water barrier properties of starch films
747 reinforced with cellulose nanocrystals obtained from sugarcane bagasse. *Carbohydrate*
748 *polymers, 110*, 53-61.

749 Sogut, E. (2020). Active whey protein isolate films including bergamot oil emulsion
750 stabilized by nanocellulose. *Food Packaging and Shelf Life, 23*, 100430.

751 Sukyai, P., Anongjanya, P., Bunyahwuthakul, N., Kongsin, K., Harnkarnsujarit, N., Sukatta,
752 U., Sothornvit, R., & Chollakup, R. (2018). Effect of cellulose nanocrystals from
753 sugarcane bagasse on whey protein isolate-based films. *Food Research International,*
754 *107*, 528-535.

755 Tian, H., Guo, G., Xiang, A., & Zhong, W.-H. (2018). Intermolecular interactions and
756 microstructure of glycerol-plasticized soy protein materials at molecular and nanometer
757 levels. *Polymer Testing, 67*, 197-204.

758 Tong, X., Luo, X., & Li, Y. (2015). Development of blend films from soy meal protein and
759 crude glycerol-based waterborne polyurethane. *Industrial Crops and Products, 67*, 11-
760 17.

761 Trifol, J., Plackett, D., Sillard, C., Szabo, P., Bras, J., & Daugaard, A. E. (2016). Hybrid poly
762 (lactic acid)/nanocellulose/nanoclay composites with synergistically enhanced barrier
763 properties and improved thermomechanical resistance. *Polymer International, 65*(8),
764 988-995.

765 Vioque, J., Alaiz, M., & Girón-Calle, J. (2012). Nutritional and functional properties of Vicia
766 faba protein isolates and related fractions. *Food Chemistry, 132*(1), 67-72.

767 Wang, X., Ullah, N., Sun, X., Guo, Y., Chen, L., Li, Z., & Feng, X. (2017). Development and
768 characterization of bacterial cellulose reinforced biocomposite films based on protein

769 from buckwheat distiller's dried grains. *International journal of biological*
770 *macromolecules, 96*, 353-360.

771 Xiang, A., Guo, G., & Tian, H. (2017). Fabrication and properties of acid treated carbon
772 nanotubes reinforced soy protein nanocomposites. *Journal of Polymers and the*
773 *Environment, 25*(3), 519-525.

774 Xie, Y., Niu, X., Yang, J., Fan, R., Shi, J., Ullah, N., Feng, X., & Chen, L. (2020). Active
775 biodegradable films based on the whole potato peel incorporated with bacterial cellulose
776 and curcumin. *International journal of biological macromolecules, 150*, 480-491.

777 Xu, X., Liu, F., Jiang, L., Zhu, J., Haagenson, D., Wiesenborn, D. P., & interfaces. (2013).
778 Cellulose nanocrystals vs. cellulose nanofibrils: a comparative study on their
779 microstructures and effects as polymer reinforcing agents. *ACS applied materials, 5*(8),
780 2999-3009.

781 Yang, F., Hanna, M. A., & Sun, R. (2012). Value-added uses for crude glycerol--a byproduct
782 of biodiesel production. *Biotechnology for biofuels, 5*(1), 1-10.

783 Ye, Z., Xiu, S., Shahbazi, A., & Zhu, S. (2012). Co-liquefaction of swine manure and crude
784 glycerol to bio-oil: Model compound studies and reaction pathways. *Bioresource*
785 *technology, 104*, 783-787.

786 Yu, Z., Sun, L., Wang, W., Zeng, W., Mustapha, A., & Lin, M. (2018). Soy protein-based
787 films incorporated with cellulose nanocrystals and pine needle extract for active
788 packaging. *Industrial Crops and Products, 112*, 412-419.

789 Zhang, S., Xia, C., Dong, Y., Yan, Y., Li, J., Shi, S. Q., & Cai, L. (2016). Soy protein isolate-
790 based films reinforced by surface modified cellulose nanocrystal. *Industrial Crops and*
791 *Products, 80*, 207-213.

792